Chapter 13

A Statistical View of Biological Dynamics

"All is flux, nothing stays still." -Heraclitus

Chapter Overview: In Which the Random Walk Model Is Applied to the Motion of Macromolecules

Dynamics in cells comes in a number of different forms. One of the most important classes of dynamical process is diffusion, the random jiggling of individual molecules in solution. When many such molecules are diffusing simultaneously, the overall concentration field undergoes changes in space and time that give the appearance of ordered and directed movements of molecules down concentration gradients. The goal of this chapter is to illustrate the important role of diffusion in living systems, to compare and contrast microscopic and continuum descriptions of diffusion and to apply these ideas to important problems such as how the method of Fluorescence Recovery After Photobleaching (FRAP) works and how receptors mediate signaling.

13.1 Diffusion in the Cell

Living systems are subject to incessant and tireless change. In the previous chapter, we eased gently into the treatment of biological dynamics by considering directed movements in water, though we relied heavily on the simplifying assumption that water can be treated as a continuous fluid rather than as a collection of interacting molecules. We are now ready to take the next step and consider the individual movements of discrete particles in water ranging from molecules to organelles to viruses and the cells they attack. Over the next four chapters, we will develop this theme of biological motions starting with the simplest case applying to nonliving and living systems alike, namely, Brownian or

diffusive motion. What makes such processes especially intriguing is that despite the stochastic microscopic underpinnings, the conspiracy formed by huge numbers of diffusing molecules over a large number of time steps can give the appearance of purposeful dynamics of particles down a concentration gradient.

As discussed in section 3.4.2 (pg. 160), Brownian motion is an inevitable outcome of the thermal jiggling of water molecules and does not indicate the activities of a living system. However, diffusive motion is always present at molecular length scales and biological systems must either tolerate, exploit or inhibit Brownian motion in order to perform directed dynamic processes. A familiar example of the physical limits put on organisms by the process of diffusion is something you experience with every breath you take. Human metabolism demands a constant high concentration of oxygen supplied to mitochondria throughout the body. Much smaller organisms that are oxygen dependent can rely simply on diffusion of oxygen as a delivery mechanism, but this is only efficient over distances of order tens of microns.

In order to grow to sizes exceeding one meter, humans and other large animals have developed elaborate mechanisms to circulate oxygen and effectively enable its delivery to all tissues. In chap. 7 we examined hemoglobin as a fascinating protein specialized for the sole purpose of carrying oxygen to parts of the body far from the lungs. Oxygen inhaled in air can diffuse through lung tissue over an effective distance of roughly 100 microns that is set not only by the free diffusion of oxygen, but also by its rate of consumption by cells in the tissue. In the lung, a fine network of capillaries surrounds each air sac and diffusion is sufficient for oxygen to travel from inhaled air to the hemoglobin filled blood in the capillaries. Rapid fluid circulation driven by your beating heart, carries the oxygen around the body much more rapidly than would be possible by simple diffusion. Reaching the tissues in the capillaries, oxygen molecules are again able to diffuse on a scale of 100 microns. This sets the constant spacing of the finest branches of capillaries for all mammals from mice to blue whales.

In this chapter we will make simple estimates about the distances over which passive transport (i.e. diffusion) is effective and derive and apply the mathematical formalism of diffusion.

13.1.1 Active versus Passive Transport

The cell is teeming with motion. One of the first questions that one might ask about all of this bustling is to what extent is it random and to what extent active and directed. As we discussed in detail in chap. 5, the interplay between thermal and deterministic forces is one of the hallmarks of cellular dynamics. On the thermal side of the ledger, one of the dominant effects of the thermal forces is the very existence of diffusive motion itself. An example of the diffusion of various ion species after the opening of an ion channel is shown in fig. 13.1.

A second example which contrasts the nature of diffusive and active transport is shown in fig. 13.2. This figure shows the motion of an RNA polymerase molecule during “free” diffusive transport within the cell as well as when it is engaged in active motion during transcription. The hallmark of directed motion

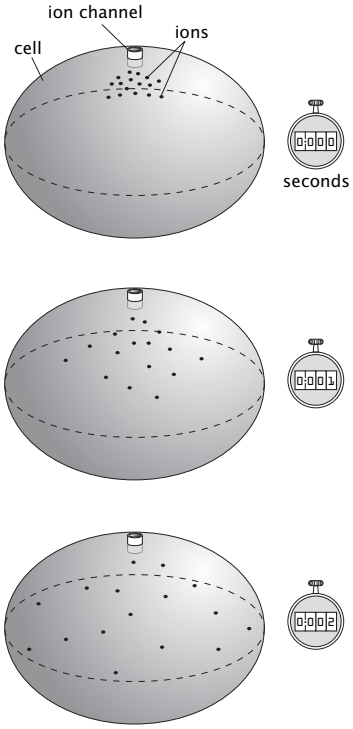

Figure 13.1: Schematic of the opening of an ion channel and the diffusion of the ions as a result. The three snapshots give a qualitative illustration of the distribution of ions as well as a depiction of the concentration as a function of position and time.

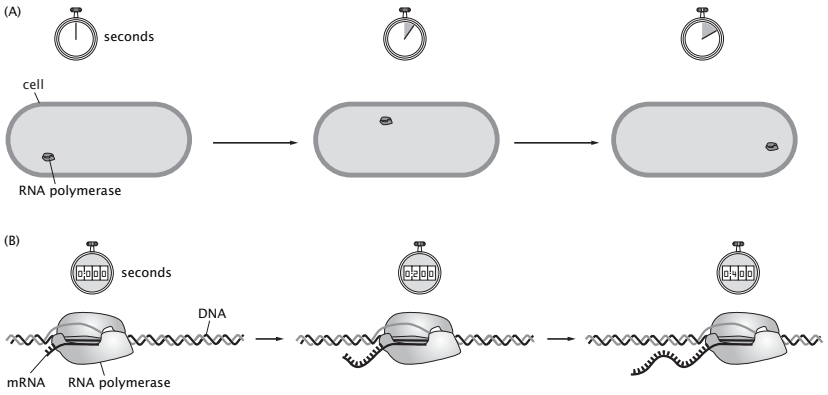

Figure 13.2: Comparison of diffusive and directed motions of RNA polymerase. (A) Free RNA polymerase molecule diffusing in a bacterial cell, (B) one-dimensional motion of RNA polymerase along DNA characteristic of active transport.

is the existence of some energy source. The key point of the figure is to contrast diffusive and directed motion. Ideas like those to be developed in this chapter are useful not only for the macromolecules of the cell, but for cells themselves. As shown in fig. 13.3, a swimming bacterium such as *E. coli* when viewed at low resolution over long times looks as though it too is undergoing a random walk characteristic of diffusive motions. On the other hand, at short time scales, it is really noticed that the cell undergoes a series of runs and tumbles as was introduced in our discussion of bacterial chemotaxis in section 4.4.4 (pg. 205). The language of random walks will be useful for thinking about a variety of different examples.

13.1.2 Biological Distances Measured in Diffusion Times

One of the simplest and most far reaching results that will emerge from the present chapter is the derivation of simple estimates for the time it takes for diffusion to transport molecules to different distances. In particular, we will show that the typical time it takes for a particle to diffuse a distance L is given by $t \simeq L^2/D$, where D is the diffusion constant of the particle. The diffusion constant has units of length^2/time, and it depends on the size of the particle, the temperature and viscosity of the surrounding fluid. We will discuss this in detail later in this chapter. For the moment, we examine the numerical consequences of this simple, but important result.

The Time It Takes a Diffusing Molecule to Travel a Distance L Grows as the Square of the Distance

Unlike in the case of ballistic motion with constant velocity where the time

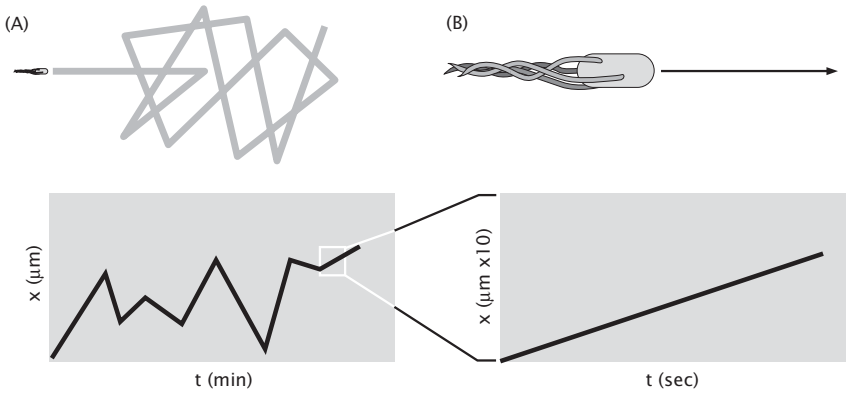

Figure 13.3: Patterns of *E. coli* swimming at different scales. (A) At low magnification, the swimming movement of a single bacterium appears to be a random walk, that is, a series of steps oriented at random angles. Plotting the x-component of the bacterial position vector as a function of time will show a chaotic series of back and forth movements. (B) At higher magnification, it is clear that each step of this random walk is made up of very straight, regular movements.

to travel a distance L grows linearly with the length scale of interest, diffusive dynamics implies that the time scale grows quadratically with distance. This result provides an opportunity for intuition building by converting distances into the corresponding diffusion time as shown fig. 13.4. In this figure, we plot the diffusion time as a function of the distance for $D = 100\ \mu\text{m}^2/\text{s}$, a characteristic diffusion coefficient for a typical globular protein in water at room temperature. Note that the time scale associated with diffusion over a distance $L \approx 10^6 \mu\text{m}$ (1 m) is 10^{10} s ($\approx$ 300 years)! This should make it clear that transport in cells and organisms requires mechanisms other than diffusion. We will come back to this point when thinking about molecular motors in chap. 16.

Diffusion Is Not Effective Over Large Cellular Distances

Though diffusion is clearly a part of the overall machinery associated with cellular dynamics, as shown in fig. 13.5, there are also instances where diffusive motion is too slow to link different regions of the cell. One of the most dramatic examples of this is illustrated by nerve cells as was already introduced in fig. 3.3 (pg. 127). In fig. 13.5(A), we show the motion of a molecule by random jiggling along an axon. Using results like those shown in fig. 13.4, it is seen that for diffusion to be effective over the meter length scale implies a time scale that is absurdly long. On the other hand, as will be seen more explicitly in coming chapters, if the molecule of interest is transported in a directed fashion by virtue of molecular motors, the time scale of the resulting motion is shortened by many orders of magnitude.

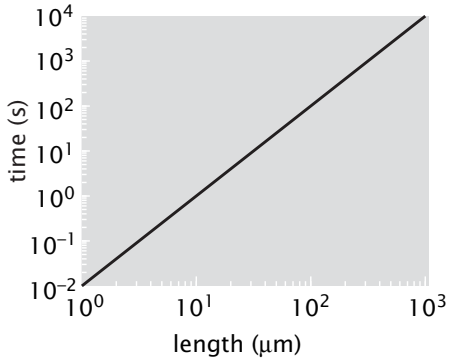

Figure 13.4: Diffusion time as a function of the distance for a typical value of the diffusion coefficient ($D = 100\ \mu\text{m}^2/\text{s}$) of a protein in water. The straight line on the log-log plot has a slope of two since time and distance are related by $t = x^2/D$.

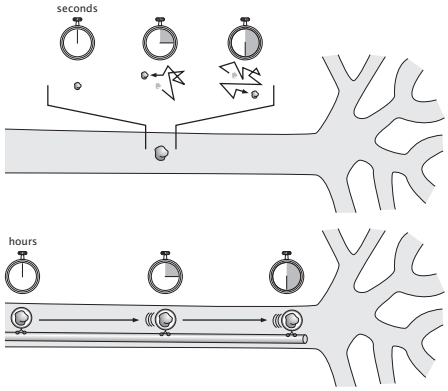

Figure 13.5: Transport within a nerve cell. (A) Passive transport of a molecule by diffusion. (B) Active transport of a molecule through directed motion of a molecular motor.

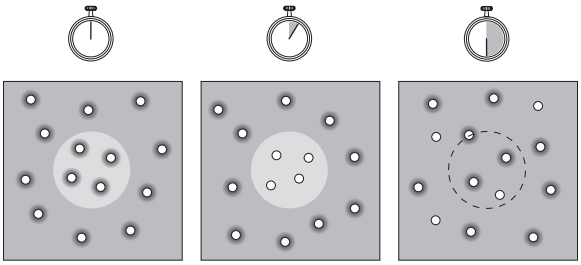

Figure 13.6: Schematic of the FRAP experiment. A particular region of the cell is photobleached, effectively destroying the fluorescent molecules in that region (as shown in the second frame). Recovery of fluorescence in the photobleached region results from fluorescent molecules from elsewhere in the sample diffusing into the photobleached region.

To better understand diffusive dynamics (especially in living cells), we need a sense of what experimental techniques can be used to probe such dynamics. In this "Experiments Behind the Facts" section, we examine several especially useful techniques.

- **Experiments Behind the Facts.** There are a number of different techniques that permit the investigation of diffusive dynamics within cells. In this box, we consider three examples of some of the ingenious techniques that have been introduced to measure diffusion: fluorescence recovery after photobleaching (FRAP), single-particle tracking and fluorescence correlation spectroscopy (FCS).

  FRAP takes advantage of the annoying feature of fluorescently labeled molecules that when they are exposed to too much light they no longer fluoresce, since the fluorophores can only emit a limited number of photons. In this instance, this weakness is turned into a strength by virtue of the fact that it can be used to measure diffusive dynamics within cells. The technique is illustrated schematically in fig. 13.6. In particular, a laser is focused on a certain spot in the cell with characteristic dimensions of a micron or larger. After the laser pulse, other fluorescently labeled molecules from elsewhere within the cell diffuse back into the space that had previously been photobleached by the laser light. By watching the time course of the recovery of fluorescence, it is possible to extract features of the diffusive dynamics.

  An example of the appearance of cells during the FRAP experiment is shown in fig. 13.7. In the series of snapshots, the bleached region shows increasing fluorescence over time as new molecules from outside the bleached region diffuse into that region in a process known as recovery. Section 13.2.3 (pg. 690) explores the mathematical foundations of this technique and describes the insights it provides.

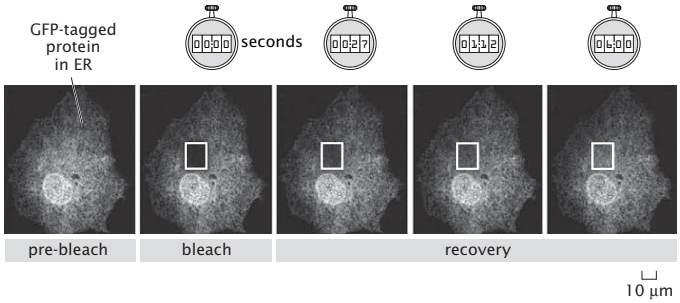

Figure 13.7: FRAP experiment showing recovery of a GFP labeled protein confined to the membrane of the endoplasmic reticulum. The boxed region is photobleached at time instant, $t = 0$. In subsequent frames, fluorescent molecules from elsewhere in the cell diffuse into the bleached region. (Adapted from J. Ellenberg *et al.*, J. Cell Biol., 138:1193, 1997.)

A more direct technique for monitoring diffusive dynamics is through explicit particle tracking in which individual trajectories are monitored. This technique is as old as the subject of Brownian motion itself, and was used as the basis of measuring atomic dimensions (and Avogadro's number) in the classic experiments of Perrin (1990). The notion of trajectory mapping is of widespread interest and has been used on problems ranging from the motions of bacteria to the wandering of individual proteins along DNA. In this case, the idea usually involves video microscopy in which images of the moving species of interest are captured at a fixed interval and the corresponding trajectory is constructed. In the bacterial setting, the nature of the trajectories of motile cells reveals that they have preferences for moving in the direction of certain nutrients, a phenomenon known as chemotaxis to be taken up in detail in chap. 19.

Another technique of great utility for probing diffusive dynamics within cells is fluorescence correlation spectroscopy (FCS). The idea of FCS is to measure the fluorescence intensity in a small region of the cell as a function of time as shown in fig. 13.8. The intensity fluctuates as the fluorescent molecules enter and leave the region under observation. By analyzing the temporal fluctuations of the intensity through the use of time dependent correlation functions, the diffusion constant and other characteristics of the molecular motion can be uncovered.

13.1.3 Random Walk Redux

The present chapter is a continuation of the story already begun in chap. 8. One of the key themes of the book is the idea that certain models have superstar status because of their ability to shed light on a range of different problems. Here we take a second look at the random walk model, a model with such hall

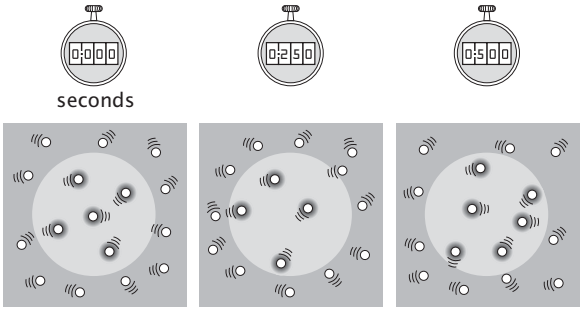

Figure 13.8: Schematic of the FCS technique. The intensity of fluorescent light coming from illuminated molecules is measured as a function of time. The intensity varies in time as a result of molecules diffusing in and out of the observation region, shown in light gray.

of fame status that it gets double billing. Recall that in chap. 8 we invoked the random walk model as a scheme for examining the structure of long chain molecules. In this chapter, we examine a second powerful role for random walk models, namely, as the basis for considering the problem of diffusion. One of the interesting contrasting perspectives that will be seen to emerge when comparing the results of chap. 8 and the present chapter is that in the earlier case, we invoked the random walk model as an *equilibrium* model. In this chapter, it is doing double time as a model of nonequilibrium dynamics.

The logic of the remainder of the chapter will be to develop the formalism of diffusive dynamics from two distinct perspectives. First, we will think in macroscopic terms by smearing out the collection of diffusing molecules into a concentration field and then by writing macroscopic evolution equations for the changes in the concentration over space and time. The second perspective will be strictly microscopic and will consider the individual hopping events of single particles as they wander aimlessly through the volume of interest (usually the cell itself). Interestingly, these two views will be reconciled as it will be seen that the conspiracy of all of the randomly wandering molecules together gives the macroscopic appearance of directed motion driven by concentration gradients. Once we have these diffusive models in hand, we will turn to a range of interesting biological applications of these ideas.

In section 5.5.2 (pg. 285), we introduced the molecular driving forces which drive a system towards equilibrium. Our argument was that if we remove some internal constraint on a system (such as those shown in fig. 5.27 (pg. 286)), the system will change until it reaches some terminal privileged state known as the equilibrium state. Prior to reaching the equilibrium state, there is an imbalance in temperature or pressure or chemical potential. For the case of mass transport of interest here, we focus on the the fact that for a system that is not in equilibrium with respect to mass transport, the chemical potential is not equal across the system and this serves as a driving force for diffusive

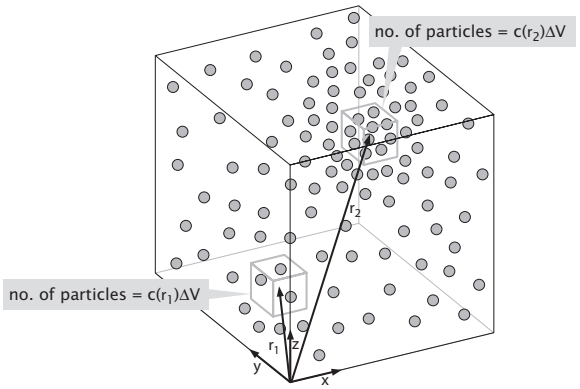

Figure 13.9: Schematic illustrating the definition of a concentration field. The system is divided up into small boxes of volume ΔV. The overall concentration field is changing sufficiently slowly that in each small box the "concentration" is constant.

motion.

13.2 Concentration Fields and Diffusive Dynamics

Our first foray into the world of diffusive dynamics will be founded upon the idea of macroscopic concentrations and fluxes. The notion of a concentration has already been used a number of times throughout the book and will continue to serve as one of the key conceptual tools for much of what happens in the remainder of the book as well. As a reminder, fig. 13.9 shows that the concentration field tells us the average number of molecules per unit volume. More precisely, the conceptual idea is that we divide space up into a bunch of small boxes (such as shown in fig. 13.9) with the boxes large enough to include many molecules, but small enough so that the density is nearly uniform over the scale of the box. We use the notation $c(\mathbf{r}, t)$ to signify the concentration in a box centered at position $\mathbf{r}$ in three-dimensional space (with units of number of particles per unit volume) and $c(x, t)$ to signify the concentration field in one-dimensional problems (with units of number of particles per unit length).

With the idea of a concentration in hand, we can consider the origins of diffusive dynamics. In particular, we begin by noting that in this macroscopic world view, diffusive dynamics is the result of concentration gradients. What we mean precisely by the term "gradient" is a spatial variation in the concentration field. Fig. 13.10 shows a simple concentration profile where on the left hand side of the domain of interest, the concentration of the molecule of interest is high while on the right hand side of the domain of interest, the concentration is low.

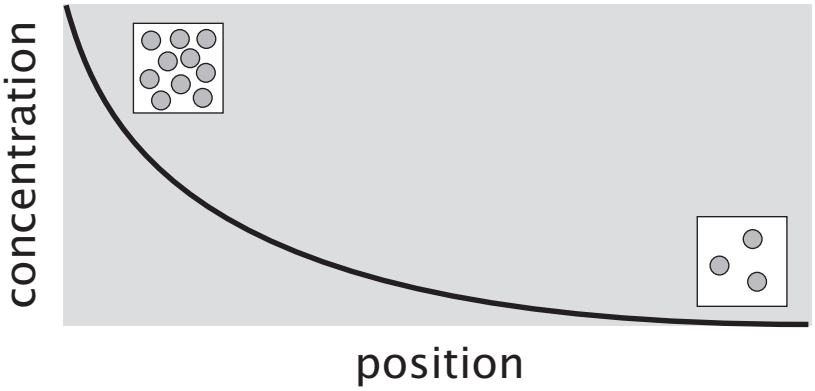

Figure 13.10: Example of a concentration profile. The plot shows the variation of the concentration with distance illustrating the idea of a position dependent concentration.

The other key quantity of interest for our macroscopic description of diffusion is the flux. Flux can be thought of conceptually as shown in fig. 13.11 where it is seen that we identify a plane with some area A and then count how many molecules cross that area per unit time. That is the component of the flux vector in that direction. In its full generality, the idea is more subtle than this since in three-dimensions, the flux is actually a vector whose components give the flux across planes that are perpendicular to the x, y and z directions. The goal of our thinking is to determine what amounts to an "equation of motion" which tells how the concentration field changes in both space and time.

Fick's Law Tells Us How Mass Transport Currents Arise as a Result of Concentration Gradients

As a first cut, we treat this problem on strictly phenomenological grounds. Later in the chapter we will show how this phenomenological law can be derived from microscopic considerations. For the time being, we restrict our attention to one dimensional concentration profiles so that the resulting mathematics is simplified. Fick's first law is the assertion that the flux is linearly related to the concentration gradient, namely,

$$j = -D\frac{\partial c}{\partial x} \tag{13.1}$$

where j is a current density per unit time, which can be thought of as the number of particles crossing unit area per unit time and where D is the diffusion coefficient. (For a brief review of partial derivatives we refer the reader to the Math Behind the Models on pg. 270.) The minus sign in Fick's law guarantees that the particle flux is in the right direction. For example, if we consider the profile shown in fig. 13.10, the concentration profile decreases with increasing

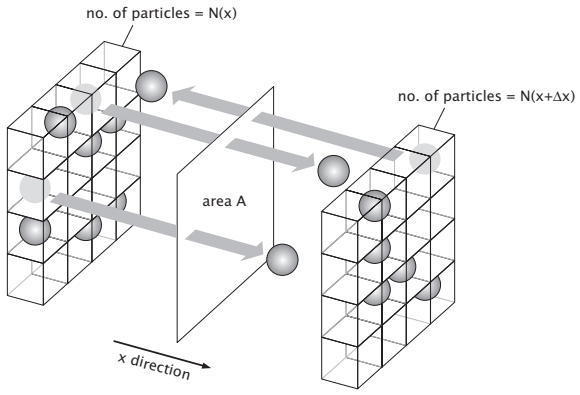

Figure 13.11: Schematic of the flux concept. In one dimension, space is discretized into a series of planes separated by a distance Δx. Particles can hop left or right and the flux across the plane between two adjacent planes is computed by counting the net number of particles crossing unit area per unit time.

x (i.e. $\partial c/\partial x < 0$). On the other hand, it's clear that molecules flow from the region of higher concentration to lower concentration, down the concentration gradient, in the positive x direction. The units of D can be determined by examining the units of all of the other quantities in Fick's law. Note that it is conventional notation to characterize the units of a quantity D as $[D]$ and the reader is asked to bear this in mind since the same notation is used to specify concentrations. Exploiting this scheme for Fick's law, we have

$$[j] = \frac{1}{L^2 T}, \tag{13.2}$$

which signifies number per unit area per unit time. The units of the right side of the equation are

$$\left[\frac{\partial c}{\partial x}\right] = \frac{\text{Number of particles}/L^3}{L} = \frac{\text{Number of particles}}{L^4}. \tag{13.3}$$

By rearranging our equation, we are left with the units of the diffusion coefficient which are $\frac{L^2}{T}$. Note that the units of the diffusion coefficient are independent of the dimensionality of space. Typical values for the diffusion constant are shown in table 13.1.

Our goal is to assess the rate at which the concentration in a small region changes over time. For concreteness, consider the box shown in fig. 13.12 where we have specialized to the case in which the flux is only in the x-direction. This means that particles are flowing in and out on the two faces of the cube that are perpendicular to the x-direction. The basic strategy is to assess how many particles enter or leave at the face at position x and similarly across the face at position $x + \Delta x$. We define $N_{box}(x, y, z, t)$ as the number of particles

Molecule	Diffusion coefficient
potassium ion in water	$\approx 2000\ \mu\text{m}^2/\text{s}$
GFP in *E.coli*	$\approx 7\ \mu\text{m}^2/\text{s}$
DNA in yeast	$5 \times 10^{-4}\ \mu\text{m}^2/\text{s}$

Table 13.1: Table of diffusion coefficients for different molecules. (Data for GFP from M. B. Elowitz *et al.*, J. Bacteriol., 181:197, 1999 and yeast data from W. F. Marshall *et al.*, Curr. Biol., 7:930, 1997.

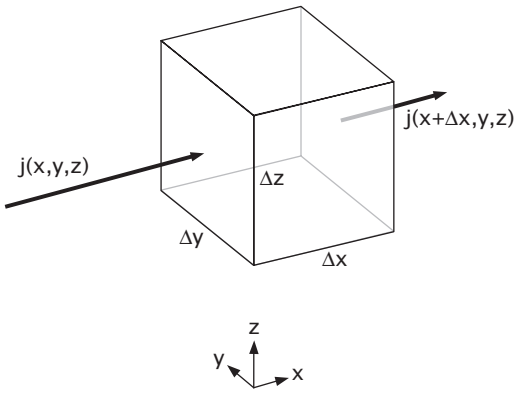

Figure 13.12: Mass transport out of a small volume element. The fluxes across the faces of the box change the number of particles in that volume.

in the box at time t and note that this can be computed as $N_{box}(x, y, z, t) = c(x, y, z, t)\Delta x\Delta y\Delta z$. Since mass is conserved (i.e. we are not yet thinking about the case where there are reactions which can alter the number of particles of a given species), the change in $N_{box}(x, y, z, t)$ can only arise from the fluxes across the faces of the box.

The Diffusion Equation Results From Fick's Law and Conservation of Mass

First, note that the change in the number of particles, N_{box}, per unit time is the change in concentration per unit time, times the volume of the box, and can be written as

$$\frac{\partial N_{box}}{\partial t} = \frac{\partial c}{\partial t}\Delta x\,\Delta y\,\Delta z. \tag{13.4}$$

By mass conservation, this result has to be equal to the number of particles going into the box per unit time, $j(x, y, z)\Delta y\,\Delta z$ *minus* the number of particles going out of the box per unit time, $j(x + \Delta x, y, z)\Delta y\,\Delta z$ and is reckoned as

$$\frac{\partial c}{\partial t}\Delta x\,\Delta y\,\Delta z = j(x, y, z)\Delta y\,\Delta z - j(x + \Delta x, y, z)\Delta y\,\Delta z. \tag{13.5}$$

We can then Taylor expand $j(x+\Delta x, y, z)$ to first order in Δx (see the discussion of Taylor expansions on pg. 273) to give

$$\frac{\partial c}{\partial t}\Delta x\,\Delta y\,\Delta z \simeq j(x,y,z)\Delta y\,\Delta z - \left[j(x,y,z) + \frac{\partial j}{\partial x}\Delta x\right]\Delta y\,\Delta z. \tag{13.6}$$

If we now collect terms, the local statement of conservation of mass can be written as

$$\frac{\partial c}{\partial t} = -\frac{\partial j}{\partial x}. \tag{13.7}$$

Note that the significance of this equation is that it is a statement about the relation between the flux and concentration in every little neighborhood of the volume of interest.

By combining the statement of mass conservation (eqn. 13.7) and the relation between flux and concentration gradient (eqn. 13.1), we can generate a very useful relation, namely,

$$\frac{\partial c}{\partial t} = D\frac{\partial^2 c}{\partial x^2}, \tag{13.8}$$

which is the classic law of diffusion in one-dimension. Note that to derive this particular form of the diffusion equation we had to assume that D is independent of concentration. This single equation embodies two key ideas: i) mass conservation and ii) a material law relating flux and concentration. Note that the first of these ideas is independent of material particulars while Fick's law need not be satisfied in all circumstances since flux might depend on concentration in a more complicated, non-linear fashion.

13.2.1 Diffusion by Summing Over Microtrajectories

The diffusion equation derived in the previous section can be obtained completely differently from a microscopic perspective. The key idea in this case is to consider the motions of individual diffusing molecules (or particles) and to sum over all of the possible microscopic trajectories of the system. The overall macroscopic response emerges as the average over all of these underlying microtrajectories. An example of one particular microtrajectory for a one-dimensional diffusion problem is shown in fig. 13.13.

Particles or fluorescently labeled molecules observed in a microscope are seen to undergo random jiggling, with each particle suffering a different trajectory. We now place these random trajectories front and center and elaborate on a quantitative treatment of diffusion that parallels the states and weights approach to computing equilibrium probabilities already used throughout the book. In later chapters we will make use of this "trajectories and weights" approach to random dynamics of diffusing particles, molecular motors, polymerization motors, etc. Here we illustrate this procedure on the simple diffusion process. The key idea is to describe a random trajectory by the probability density for finding a particle at a particular position at a given instant in time, $p(\mathbf{x}, t)$. In particular, the probability of finding the particle in a box of width Δx centered

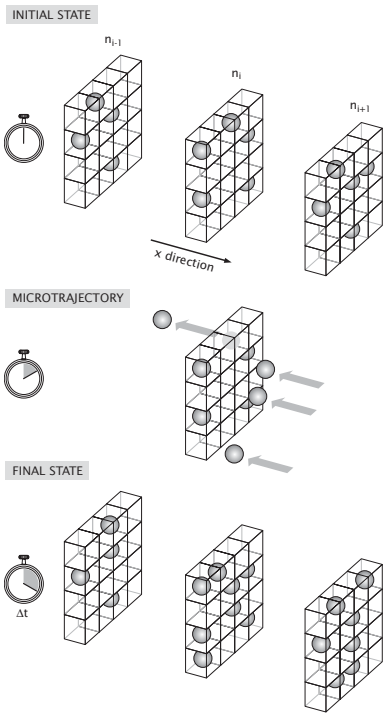

Figure 13.13: Schematic of a one-dimensional array of random walkers. Space is discretized into a set of planes.

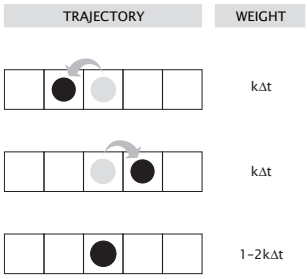

Figure 13.14: Trajectories and weights for simple diffusion. A given diffusing particle can do one of three things at every time step: jump left, jump right or stay put. Each of these microtrajectories has an associated statistical weight.

at point x at time t is given by $p(x,t)\Delta x$. To simplify the math we specialize to one-dimensional motion, and discretize space and time. In this case, particle trajectories can be compactly denoted as long lists of integers which specify the position of the particle in units of a at different instants of time, measured in units of Δt. To derive the governing equation for the probability $p(x,t)$ we only have to specify the weights of all realizations of microtrajectories that can occur over time Δt.

Microtrajectories and their corresponding weights are shown in fig. 13.14. The diffusing particle, over time Δt, either stays put, or jumps to the left or right a distance a, where we imagine that the particles can only occupy lattice sites on a lattice with spacing a. The probability of making a jump in either direction is $k\Delta t$, while the probability of staying put is $1-2k\Delta t$, assuring that the probabilities for all three possible outcomes add up to one. We can use this model to compute a number of quantities associated with the particle trajectories. We begin by computing the mean and the variance of the particle displacement over time t. In time t the particle makes a total of $N = t/\Delta t$ steps, each accompanied by a displacement Δx_i, $i = 1, 2, \cdots N$. The total displacement $\Delta x_{\rm tot} = \Delta x_1 + \Delta x_2 + \cdots \Delta x_N$, is a sum of independent identically distributed random variables. Therefore, as shown in the "Tricks Behind the Math" box at the end of this section, the mean and the variance of $\Delta x_{\rm tot}$ are simply N times the mean and variance of Δx, the displacement for one time step. These are readily calculated from fig. 13.14 by summing over microtrajectories. We obtain the mean by summing over the three microtrajectories that can occur during a given time step as

$$\langle \Delta x \rangle = a \times k\Delta t + (-a) \times k\Delta t + (0) \times (1 - 2k\Delta t) = 0. \qquad (13.9)$$

We can compute the variance as the average of the square of displacement once

again by summing over all of the eventualities at a given instant as

$$\left\langle \Delta x^2 \right\rangle = a^2 \times k\Delta t + (-a)^2 \times k\Delta t + (0)^2 \times (1 - 2k\Delta t) = 2a^2 k\Delta t. \quad (13.10)$$

The variance of the total displacement is $N = t/\Delta t$ times greater resulting in

$$\left\langle \Delta x_{\text{tot}}^2 \right\rangle = 2(a^2 k)\, t \quad (13.11)$$

which is the result for diffusive spreading if we identify $a^2 k$ with the diffusion constant D.

The trajectories and weights approach can also be used to derive the governing equation for $p(x,t)$, the probability density that the particle is at position x at time t. The idea is to sum over all the microtrajectories starting at time instant t that result in the particle being at position x at time $t + \Delta t$. For this to happen the particle needs to be at position x (if it is to stay put on the next time step), $x - a$ (if it is to jump to the right at the next time step), or $x + a$ (if it is to jump to the left at the next time step) at time t, and the associated probabilities are $p(x,t)$, $p(x-a,t)$, and $p(x+a,t)$, respectively. Using the probabilities in fig.13.14, we can write $p(x, t + \Delta t)$ as a sum over microtrajectories,

$$p(x,t+\Delta t) = \underbrace{(1-2k\Delta t)\times p(x,t)}_{\text{stay put}} + \underbrace{k\Delta t \times p(x-a,t)}_{\text{jump right}} + \underbrace{k\Delta t \times p(x+a,t)}_{\text{jump left}} \quad (13.12)$$

which leads to a discrete differential (or, difference) equation for $p(x,t)$. Also, in writing the above equation we have used the so-called Markov property of the process, namely the fact that the probability of a microtrajectory at time t is independent of the previous history of the particle; this is what allows us to express the probability of each outcome as a product of probabilities. To arrive at the more familiar, continuous diffusion equation we once again make use of the Taylor expansion

$$\begin{aligned} p(x,t+\Delta t) &\approx p(x,t) + \Delta t \frac{\partial p(x,t)}{\partial t} \\ p(x \pm a, t) &\approx p(x,t) \pm a\frac{\partial p(x,t)}{\partial x} + \frac{a^2}{2}\frac{\partial^2 p(x,t)}{\partial x^2}\ . \end{aligned} \quad (13.13)$$

Substituting these formulas into eqn.13.12 gives

$$\frac{\partial p(x,t)}{\partial t} = (a^2 k)\frac{\partial^2 p(x,t)}{\partial x^2}\ . \quad (13.14)$$

This is the diffusion equation derived in the previous section from Fick's law, with $D = a^2 k$, the same identification we made above.

Like with many fundamental results, there are multiple ways of deriving the diffusion equation. It is instructive to examine yet another way of deriving this equation which is another way of summing over all of the microscopic trajectories available to the system at every instant. The approach adopted here is that

taken by Einstein in one of his classic 1905 papers. We imagine that time is sliced up into intervals of length Δt and that at every time step, particles can either jump or stay put. Einstein starts by writing the concentration at position x and time $t + \Delta t$ as the following integral

$$\underbrace{c(x, t + \Delta t)}_{\text{concentration at } x \text{ now}} = \int_{-\infty}^{+\infty} \underbrace{c(x + \Delta, t)}_{\text{concentration at } x+\Delta \text{ earlier}} \underbrace{\phi(\Delta)}_{\text{probability of a jump of length } \Delta} d\Delta. \tag{13.15}$$

What this integral says precisely is that to find the concentration at position x at time $t + \Delta t$ we need to sum over all of the possible ways that particles could have gotten there. In particular, at time t, the particle could have been at position $x + \Delta$ and then jumped to position x during the time step. (Note: we follow Einstein's notation precisely, so the reader is warned that what Einstein calls Δ is our Δx in our earlier derivation of the diffusion equation). The microtrajectory that we described above can be true for any choice of Δ. This means that in order to obtain the concentration at x we have to sum over all of the possible jumping events with each one weighted by $\phi(\Delta)$, the probability of jumping a distance Δ. Effectively, Einstein considers the possibility that particles can jump *any* distance, whereas in our earlier derivation, we permitted jumps only of size a. Einstein makes two further assumptions. First, he posits a symmetry in the jump probabilities of the form

$$\phi(\Delta) = \phi(-\Delta), \tag{13.16}$$

which states that the probability of jumping a certain distance to the right is the same as the probability of jumping that same distance to the left, i.e. that there is no bias in the chosen direction. If we included a bias we would get a driven diffusion equation, which we will encounter in the context of molecular motors. The other key feature of the distribution $\phi(\Delta)$ is

$$\int_{-\infty}^{+\infty} \phi(\Delta)\, d\Delta = 1, \tag{13.17}$$

which guarantees that the molecules do *something* at every time step. We now make a familiar refrain by Taylor expanding both terms appearing in eqn. 13.15, which results in

$$c(x, t + \Delta t) \simeq c(x, t) + \frac{\partial c}{\partial t}\Delta t \tag{13.18}$$

and

$$c(x + \Delta, t) \simeq c(x, t) + \frac{\partial c}{\partial x}\Delta + \frac{1}{2}\frac{\partial^2 c}{\partial x^2}\Delta^2. \tag{13.19}$$

If we now substitute these results into eqn. 13.15 we find

$$c(x,t)+\frac{\partial c}{\partial t}\Delta t \simeq c(x,t)\int_{-\infty}^{+\infty}\phi(\Delta)\,d\Delta+\frac{\partial c}{\partial x}\int_{-\infty}^{+\infty}\Delta\cdot\phi(\Delta)\,d\Delta+\frac{1}{2}\frac{\partial^2 c}{\partial x^2}\int_{-\infty}^{+\infty}\Delta^2\phi(\Delta)\,d\Delta. \tag{13.20}$$

The right hand side of this equation can be examined term by term. The integral in the first term is one by eqn. 13.17. As a result, we have a term of the form $c(x,t)$ on both sides of the equation that will cancel out of the final result. The second term is zero because we are integrating an odd function, Δ, times an even function, $\phi(\Delta)$. If we define the integral in the last term as

$$D \equiv \frac{1}{2\Delta t}\int_{-\infty}^{+\infty} \Delta^2 \phi(\Delta)\, d\Delta \tag{13.21}$$

we can write equation 13.21 as

$$\frac{\partial c}{\partial t} = D\frac{\partial^2 c}{\partial x^2} \tag{13.22}$$

which is precisely the same result for the one-dimensional diffusion equation that we obtained earlier.

- **The Tricks Behind the Math: Averaging Sums of Variables.** Independent identically distributed random variables $\sigma_1, \sigma_2, \ldots, \sigma_N$ all have the same probability distribution, $P(\sigma)$, and their joint probability distribution factorizes,

$$P_{\text{joint}}(\sigma_1, \sigma_2, \ldots, \sigma_N) = P(\sigma_1) \times P(\sigma_2) \times \ldots \times P(\sigma_N)\ . \tag{13.23}$$

The factorization property simply means that the probability that one of the random variables takes on a particular value is independent of all the other random variables in the bunch. If the variables σ_i take on two values, say 1 and 0, this mathematical construct could be used, for example, to describe N non-interacting ion-channels, with 0 and 1 corresponding to a channel being closed or open. Beyond this example there are many more that we will encounter so we take a brief interlude here to derive two useful identities for the sum of independent identically distributed random variables.

We begin by showing that the average value of the sum, $\sigma_1+\sigma_2+\ldots+\sigma_N$, is equal to N times the average of one of the random variables (since they are identical, it doesn't matter which one we choose). We start by writing the average of the sum using the joint probability distribution:

$$\left\langle \sum_{i=1}^{N} \sigma_i \right\rangle = \sum_{\sigma_1}\sum_{\sigma_2}\cdots\sum_{\sigma_N} \left[\sum_{i=1}^{N} \sigma_i P_{\text{joint}}(\sigma_1, \sigma_2, \ldots, \sigma_N)\right]\ ; \tag{13.24}$$

Then, we make use of the factorization property given in eqn. 13.23, and the above equation can be written as

$$\begin{aligned}\left\langle \sum_{i=1}^{N} \sigma_i \right\rangle \quad = \quad & \sum_{\sigma_1}\sigma_1 P(\sigma_1)\sum_{\sigma_2} P(\sigma_2)\ldots\sum_{\sigma_N} P(\sigma_N) + \\ & \sum_{\sigma_1} P(\sigma_1)\sum_{\sigma_2}\sigma_2 P(\sigma_2)\ldots\sum_{\sigma_N} P(\sigma_N) + \ldots \\ & \sum_{\sigma_1} P(\sigma_1)\sum_{\sigma_2} P(\sigma_2)\ldots\sum_{\sigma_N}\sigma_N P(\sigma_N)\end{aligned} \tag{13.25}$$

Finally, using the fact that all the probabilities must add up to one ($\sum_\sigma P(\sigma) = 1$) and the fact that all the random variables are identical, we arrive at the desired result, namely,

$$\left\langle \sum_{i=1}^{N} \sigma_i \right\rangle = N \sum_{\sigma} \sigma P(\sigma) = N \left\langle \sigma \right\rangle \ . \tag{13.26}$$

Next, we compute the variance of the sum of N independent identically distributed random variables. The variance is the average of the square of the difference between the random variable and its mean

$$var \sum_{i=1}^{N} \sigma_i = \left\langle \left[\sum_{i=1}^{N} \sigma_i - \left\langle \sum_{i=1}^{N} \sigma_i \right\rangle \right]^2 \right\rangle \ . \tag{13.27}$$

Using the average computed above, and expanding the square using the binomial formula, $(a-b)^2 = a^2 - 2ab + b^2$, we can simplify the above equation to read

$$var \sum_{i=1}^{N} \sigma_i = \left\langle \left[\sum_{i=1}^{N} \sigma_i \right]^2 \right\rangle - N^2 \left\langle \sigma \right\rangle^2 \ . \tag{13.28}$$

Writing the square in the above equation as a product of two equal terms, and being mindful of using different summation variables i and j in the two sums, we arrive at

$$var \sum_{i=1}^{N} \sigma_i = \left\langle \sum_{i,j=1}^{N} \sigma_i \sigma_j \right\rangle - N^2 \left\langle \sigma \right\rangle^2 \ . \tag{13.29}$$

Now, to compute $\left\langle \sum_{i,j=1}^{N} \sigma_i \sigma_j \right\rangle$ we break up the double sum into two pieces, one with N terms where $i = j$, and the other with the remaining $N^2 - N$ terms where $i \neq j$:

$$\left\langle \sum_{i,j=1}^{N} \sigma_i \sigma_j \right\rangle = \left\langle \sum_{i=1}^{N} \sigma_i^2 \right\rangle + \left\langle \sum_{i \neq j; i,j=1}^{N} \sigma_i \sigma_j \right\rangle \tag{13.30}$$

Since all the σ_i's are independent, for $i \neq j$ we have $< \sigma_i \sigma_j >=< \sigma_i >< \sigma_j >=< \sigma >^2$. Putting all this back into eqn.(13.29), we arrive at the result

$$var \sum_{i=1}^{N} \sigma_i = N \left\langle \sigma^2 \right\rangle + (N^2 - N) \left\langle \sigma \right\rangle^2 - N^2 \left\langle \sigma \right\rangle^2 \ = N \left[\left\langle \sigma^2 \right\rangle - \left\langle \sigma \right\rangle^2 \right] = N \ var(\sigma). \tag{13.31}$$

In other words, the variance of the sum of N independent identically distributed random variables is equal to N times the variance of one.

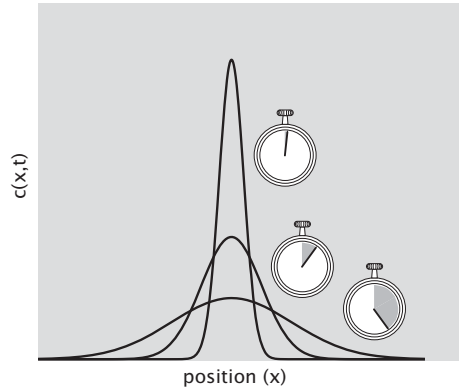

Figure 13.15: Time evolution of the concentration field. The plot shows the solution for the diffusion equation at different times for an *initial* concentration profile that is a spike at $x = 0$.

13.2.2 Solutions and properties of the diffusion equation

Concentration Profiles Broaden Over Time in a Very Precise Way

Now that we have the diffusion equation in hand, it is of great interest to examine its biological consequences. One of the most useful tools corresponds to knowing how to solve this equation for a spike of concentration at the origin at time $t = 0$. In particular, if at time $t = 0$ we start with N molecules in an infinitesimally small region around $x = 0$, the concentration profile will evolve in the following way

$$c(x,t) = \frac{N}{\sqrt{4\pi Dt}} e^{-\frac{x^2}{4Dt}}. \tag{13.32}$$

The solution itself is left to the problems at the end of the chapter. Further, by dividing by c_0, this equation can then be interpreted as giving the probability density for finding a particle between x and $x+dx$. The solution quoted above is often denoted as the Green's function of the diffusion equation and its evolution can be seen in fig. 13.15. This equation for the concentration tells us that the profile has the form of a Gaussian. The width of the Gaussian is $4Dt$ and hence, it increases linearly with time. One of the most beautiful features of a solution like this is that once it is known, by exploiting the linearity of the diffusion equation itself, we are then free to write the solution for an arbitrary initial distribution of diffusing molecules. This idea will be taken up in the problems at the end of the chapter.

Note in fig. 13.15 that the mean position of the concentration distribution does not change with time. This corresponds to the absence of a drift term, though drift terms will form a centerpiece of our discussion in chap. 16 when we turn to the dynamics of molecular motors. On the other hand, even in

the absence of drift, the diffusive dynamics are rich and interesting. One of the most interesting quantities to feature is the width of the distribution, $\langle x^2 \rangle$, which broadens over time. Since the distribution is Gaussian, we can essentially read off the dynamics of the width, but we take this opportunity to compute it explicitly since it is instructive both physically and mathematically. To compute this broadening, we need to evaluate $\langle x^2 \rangle$ as

$$\langle x^2 \rangle = \frac{\int_{-\infty}^{+\infty} x^2 \frac{N}{\sqrt{4\pi Dt}} e^{-\frac{x^2}{4Dt}} \, dx}{N} = \frac{1}{\sqrt{4\pi Dt}} \int_{-\infty}^{+\infty} x^2 e^{-\frac{x^2}{4Dt}} \, dx, \tag{13.33}$$

where we made use of the probability distribution for finding a particle at position x at time t, which is related to the concentration distribution, eqn. 13.32, by $c(x,t)/N$. Using the trick introduced in the "Tricks Behind the Math" box below, we can evaluate this integral straightaway to find

$$\langle x^2 \rangle = \frac{1}{\sqrt{4\pi Dt}} \int_{-\infty}^{+\infty} x^2 e^{-\frac{x^2}{4Dt}} \, dx = \frac{1}{\sqrt{4\pi Dt}} \frac{\sqrt{\pi}}{2} (4Dt)^{3/2} = 2Dt. \tag{13.34}$$

Note that this is the key result that we have already invoked a number of times (for example, see section 13.1.2 on pg. 672) throughout the book as the basis of intuition about diffusive processes. In particular, this is the result that we have argued reveals how diffusion times scale with the square of the distance over which diffusion must act.

- **The Tricks Behind the Math: Differentiating With Respect to a Parameter.** Sometimes the knowledge of one integral in terms of a parameter appearing in the integrand can be used to compute a number of related integrals obtained by differentiating with respect to the parameter in question. Indeed, we already invoked this trick in our discussion of the partition function (pg. 307. In the case of the Gaussian integral (discussed on pg. 334),

$$\int_{-\infty}^{\infty} e^{-\alpha x^2} \, dx = \sqrt{\frac{\pi}{\alpha}}, \tag{13.35}$$

we can differentiate both sides of the equation with respect to the parameter α to obtain

$$\int_{-\infty}^{+\infty} x^2 e^{-\alpha x^2} \, dx = -\frac{\partial}{\partial \alpha} \int_{-\infty}^{+\infty} e^{-\alpha x^2} \, dx = -\frac{\partial}{\partial \alpha} \sqrt{\frac{\pi}{\alpha}} = \frac{\sqrt{\pi}}{2\alpha^{3/2}} \, . \tag{13.36}$$

Further differentiation with respect to α leads to result for integrals with x to any even power in the integrand.

13.2.3 FRAP and FCS

One of the merits of the techniques described earlier in the chapter (pg. 675) for measuring diffusion is that they can be readily applied to living cells. The diffusive behavior of a molecule in the environment of a cell will depend upon the

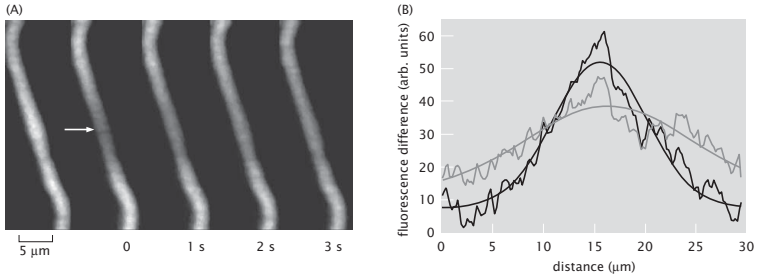

Figure 13.16: FRAP data from a bacterium labeled with green fluorescent protein. (A) The images show an elongated bacterium with the prebleach image on the left and subsequent images taken at different times (reported in seconds) after photobleaching. The arrow shows the photobleached region. (B) The curves shows the difference in intensity before and after photbleaching, along the long axis of the bacterium. The black curve is measured right after photobleaching while the gray curve was obtained from an image acquired four seconds later. (Adapted from C. W. Mullineaux *et al.*, J. Bacteriol., 188:3442, 2006.)

physical structure of the molecule itself and also on the structure of its environment as well as its interactions with other molecules. In the following chapter we will explore some specific cases of how information can be gleaned about cell structure by examining deviations from the diffusive behavior expected in dilute solutions. Here we start with a simple experimental case examining the motion of tracer molecules such as the green fluorescent protein (GFP) within living cells where the tracer molecule does not form any specific binding reactions with cellular constituents. An example of this sort of experiment is shown in fig. 13.16 for an experiment in which elongated *E. coli* cells are photobleached and the resulting fluorescence intensity is measured over time.

To calculate the expected time evolution of GFP following photobleaching, consider a one-dimensional *E. coli* such as might be found in the gut of a spherical cow (see fig. 20.2 (pg. 1083)). We leave the more realistic two-dimensional problem to the end of the chapter, though we note that the key features of the problem are already revealed in the one-dimensional case. We consider a one-dimensional model of a FRAP experiment. The fluorescent molecules diffuse in a box of length $2L$, which for convenience we place between $-L$ and L along the x-axis. The initial concentration is equal to c_0 on the intervals $-L < x < -a$ and $a < x < L$ and is zero on the interval $-a < x < a$ as is shown in fig. 13.17. In other words we imagine that we start with a uniform concentration c_0 of fluorescent molecules in the width-$2L$ box and then we photobleach all the molecules in a smaller box of size $2a$ by exposing them to intense laser light. If we were to look under a microscope we would observe the recovery of fluorescence as the non-bleached molecules made their way into the box of size $2a$. Based on the speed of fluorescence recovery the diffusion constant of the fluorescent molecules

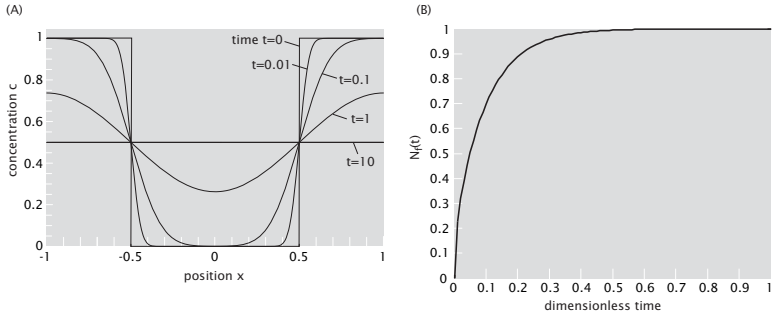

Figure 13.17: One-dimensional model of Fluorescence Recovery After Photobleaching (FRAP). (A) Concentration profile for different times after photobleaching. The bleached region is half the size of the confining region, $2L$. (B) Fluorescence recovery as a function of time for different sizes of bleached regions. Recovery is fastest when the bleached region is half the size of the confining region. In both graphs, time is measured in units of L^2/D and length in units of L.

can be measured.

We can use the simple one-dimensional model to gain quantitative insight into the recovery process. To compute the recovery curves we first solve the diffusion equation,

$$\frac{\partial c}{\partial t} = D\frac{\partial^2 c}{\partial x^2} \tag{13.37}$$

for the concentration of fluorescent molecules $c(x,t)$, with the initial concentration after photobleaching given by

$$c(x,0) = \begin{cases} c_0 & \text{for } -L < x < -a \\ 0 & \text{for } -a < x < a \\ c_0 & \text{for } a < x < L \end{cases} \tag{13.38}$$

We also impose the boundary condition $\partial c/\partial x = 0$ for $x = \pm L$ which says that the flux of fluorescent molecules vanishes at the boundaries of the one-dimensional cell (no material flows in or out). This mimics the real-life situation with fluorescent proteins confined to the volume of the cell, to the cell membrane, or some other sub-cellular structure.

To solve the diffusion equation with the prescribed initial and boundary conditions we begin by expanding the concentration profile, $c(x,t)$, in terms of cosine functions (introduced in the "Math Behind the Models" on pg. 420),

$$c(x,t) = A_0(t) + \sum_{n=1}^{\infty} A_n(t)\cos\left(\frac{x}{L}n\pi\right) \ . \tag{13.39}$$

This expansion guarantees that the boundary conditions are met, namely each of the functions $A_n(t)\cos(xn\pi/L)$ has vanishing first derivatives at $x = \pm L$.

Furthermore, since the initial concentration profile takes the same values for positive and negative x, it is readily expanded in cosine functions. The solution of the diffusion equation now boils down to finding the functions $A_n(t)$ such that both eqn. 13.37 and the initial condition, eqn. 13.38 are satisfied.

To proceed, we substitute the series expansion of $c(x,t)$ into the diffusion equation. This yields,

$$\frac{\partial A_0}{\partial t} + \sum_{n=1}^{\infty} \frac{\partial A_n(t)}{\partial t} \cos\left(\frac{x}{L} n\pi\right) = D \sum_{n=1}^{\infty} \left(-A_n(t) \frac{n^2\pi^2}{L^2}\right) \cos\left(\frac{x}{L} n\pi\right) \quad (13.40)$$

which due to the orthogonality property of the cosine functions for different n (see eqn. 13.44 below) turns into a set of independent differential equations

$$\begin{aligned} \frac{\partial A_0}{\partial t} &= 0 \\ \frac{\partial A_n}{\partial t} &= -\frac{Dn^2\pi^2}{L^2} A_n(t) \quad (n \geq 1) \ . \end{aligned} \quad (13.41)$$

The solution to each one of these (infinite in number) equations is an exponential function

$$A_n(t) = A_n(0) e^{-\frac{Dn^2\pi^2}{L^2} t} \quad (13.42)$$

which when substituted into eqn.(13.39) gives

$$c(x,t) = A_0(0) + \sum_{n=1}^{\infty} A_n(0) e^{-\frac{Dn^2\pi^2}{L^2} t} \cos\left(\frac{x}{L} n\pi\right) \ . \quad (13.43)$$

The final piece of the puzzle is the determination of the constants $A_n(0)$.

To compute the initial amplitudes of the cosine functions we once again resort to the orthogonality property of these functions

$$\int_{-L}^{L} \cos\left(\frac{x}{L} n\pi\right) \cos\left(\frac{x}{L} m\pi\right) dx = L\delta_{n,m} \ . \quad (13.44)$$

In particular we multiply both sides of eqn. 13.43 with $\cos\left(\frac{x}{L} n\pi\right)$, for different values of n, and then integrate over x, which provides us with the equations

$$\begin{aligned} A_0(0) &= \frac{1}{2L} \int_{-L}^{L} c(x,0) dx \\ A_n(0) &= \frac{1}{L} \int_{-L}^{L} c(x,0) \cos\left(\frac{x}{L} n\pi\right) dx \quad (n \geq 1) \ , \end{aligned} \quad (13.45)$$

for the initial amplitudes. Substituting the initial concentration profile, $c(x,0)$, into these equations, and after performing the integrals, we arrive at

$$\begin{aligned} A_0(0) &= c_0 \ \frac{L-a}{L} \\ A_n(0) &= -2c_0 \ \frac{\sin(n\pi a/L)}{n\pi} \quad (n \geq 1) \ . \end{aligned} \quad (13.46)$$

Putting these results back into the derived formula for $c(x,t)$, eqn. 13.43 gives us the solution for the concentration profile as a function of time,

$$c(x,t) = c_0 \left[1 - \frac{a}{L} - \sum_{n=1}^{\infty} \frac{2\sin(n\pi a/L)}{n\pi} e^{-\frac{Dn^2\pi^2}{L^2}t} \cos\left(\frac{x}{L} n\pi\right) \right] , \qquad (13.47)$$

which is plotted as a function of x for different times (and setting $a = L/2$) in fig. 13.17(A). Note that at long times, such that t is much greater than L^2/D, which is the diffusion time for a box of length L, the concentration profile tends to a constant value equal to $c_\infty = c_0(1 - a/L)$. This can be understood in a very simple way. Namely, at long times we expect diffusion to make the concentration profile uniform over the $2L$ interval. Then, the fact that the number of fluorescent molecules does not change in time leads to the equation,

$$c_\infty(2L) = c_0[2(L - a)] \qquad (13.48)$$

which gives the computed value of the concentration at long times.

Given the concentration profile as a function of time we are now in the position to compute a FRAP recovery curve within our simple one-dimensional model. We ask, how many fluorescent molecules are there in the bleached region as a function of time? In our simple model the bleached region is a box that spans from $-a$ to a on the x-axis. We already know that at $t = 0$, the number of fluorescent molecules in the bleached region is $N_f = 0$ while at times much longer than the diffusion time this number will tend to $c_\infty(2a)$. For intermediate times we need to compute

$$N_f(t) = \int_{-a}^{a} c(x,t)dx \ . \qquad (13.49)$$

Substituting our result for the concentration profile given in eqn. 13.47 into the integral leads to an expression for the recovery curve:

$$N_f(t) = 2c_0 a(1 - \frac{a}{L}) \left[1 - \frac{1}{a/L(1 - a/L)} \sum_{n=1}^{\infty} \frac{2}{n^2\pi^2} \ \sin^2(n\pi a/L) e^{-\frac{Dn^2\pi^2}{L^2}t} \right] . \qquad (13.50)$$

Note that at very long times N_f approaches $c_\infty(2a) = 2c_0 a(1 - a/L)$, as expected.

In fig. 13.17(B) we plot a FRAP recovery curve normalized by $2c_0 a(1-a/L)$, the total number of fluorescent molecules in the bleached region in the long time limit. The model makes an interesting prediction that the recovery is fastest when the size of the bleached region is equal to half the size of the confining region. Furthermore, the recovery curves are identical for bleached regions of fractional size a/L and $1 - a/L$, which follows directly from eqn. 13.50. In particular, the right hand side of this equation is invariant under exchange $a/L \leftrightarrow 1 - a/L$.

13.2.4 Drunks on a Hill: The Smoluchowski Equation

Thus far, our treatment of diffusion has been based upon those problems in which there are no external forces acting on the particle of interest. On the other hand, there are a number of diffusive processes in which the diffusing species is subjected to a force. For example, we can imagine ion diffusion in the presence of an electric field. In the trajectories and weights treatments of diffusion we assumed that the probability of jumping in any of the allowed directions is equal. This is not the case if an external applied force biases the motion of the particle in some particular direction. In this case we expect the rates to be asymmetrical since a jump in the direction of the force will be more probable than a jump against the direction of the force. To see the effect of this asymmetry we can repeat the analysis which led to the derivation of the diffusion equation, but now with the force-induced asymmetry in jump rates.

First we compute the mean and the variance of the particle displacement after time t. Once again, both the mean and variance of the total displacement are $N = t/\Delta t$ times greater than the mean and variance of the displacement Δx resulting from a single time step. These in turn are readily computed from the trajectories and weights as shown in fig. 13.18, resulting in

$$\begin{aligned} \langle \Delta x \rangle &= a \times k_+ \Delta t + (-a) \times k_- \Delta t = a(k_+ - k_-)\Delta t \\ \mathrm{var}(\Delta x) &= a^2 \times k_+ \Delta t + (a)^2 \times k_- \Delta t - \langle \Delta x \rangle^2 = a^2(k_+ + k_-)\Delta t \end{aligned} \tag{13.51}$$

where in obtaining the final result for the variance we have dropped the $\langle \Delta x \rangle^2$ term on account of it being much smaller than the first one; this is because the term that is omitted is quadratic in Δt, or, more precisely, because $k_\pm \Delta t \ll 1$.

We see that the variance of the displacement is same as for unbiased diffusion, with the diffusion constant now being given by $D = (k_+ + k_-)a^2/2$. On the other hand, the mean is now non-zero, and it increases linearly with time. Therefore, the overall motion of the particle can be described as diffusion with drift, with a drift velocity

$$v = \frac{\langle \Delta x \rangle}{\Delta t} = a(k_+ - k_-) \ . \tag{13.52}$$

Note that for a particle moving through a fluid, and in the limit of low-Reynolds number, the drift velocity is related to the applied force on the particle, $F = \gamma v$, with γ the friction coefficient. This idea was already discussed in section 12.4.1 (pg. 648).

Just as we did for the unbiased diffusion case, we can use the trajectories and weights approach to derive the governing equation for $p(x,t)$, the probability density of finding a particle at position x at time t. Again, we consider all the microtrajectories that in time Δt end up at position x. There are three such trajectories, with the particle being initially at x and staying put, the particle starting at $x - a$ and jumping to the right, and finally, the particle starting at $x + a$ and jumping to the left. The probability $p(x, t + \Delta t)$ is given by the sum

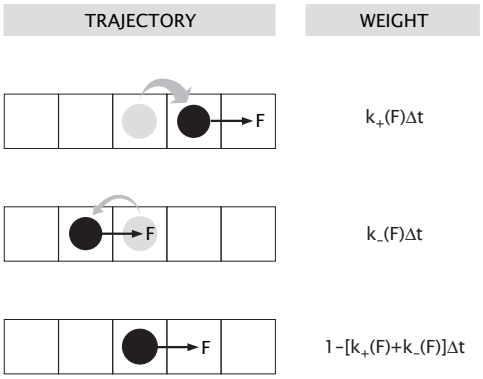

Figure 13.18: Trajectories and weights for driven diffusion. The probability of jumping to the left and right are unequal since jumping in the direction of the force is more likely than jumping opposite the direction of the applied force.

over these trajectories,

$$p(x,t+\Delta t) = [1-(k_+ + k_-)\Delta t] \times p(x,t) + k_+ \Delta t \times p(x-a,t) + k_- \Delta t \times p(x+a,t) \; . \tag{13.53}$$

We can turn this difference equation into the more familiar continuum form by Taylor expanding, $p(x, t + \Delta t)$ and $p(x \pm a, t)$, as was done in eqn. 13.13. We arrive at

$$\frac{\partial p(x,t)}{\partial t} = -v\frac{\partial p(x,t)}{\partial x} + D\frac{\partial^2 p(x,t)}{\partial x^2} \; . \tag{13.54}$$

with the drift velocity $v = a(k_+ - k_-)$ and diffusion coefficient $D = (k_+ + k_-)a^2/2$, as stated above.

13.2.5 The Einstein Relation

The microscopic derivation of diffusion with drift given above can be complemented by a macroscopic derivation. As we will see below, this leads to an important relation between diffusion and friction first derived by Einstein. We consider a generalization of Fick's law to account for the bias that will arise in the presence of driving forces. In particular, a force F exerted on a particle results in a drift velocity $v = F/\gamma$, where γ is the friction coefficient. For a spherical particle of radius a moving through a fluid of viscosity η, $\gamma = 6\pi\eta a$. (See eqn. 12.32 and accompanying discussion on pg. 652.) The presence of a net drift of a collection of particles all moving with the same mean velocity v,

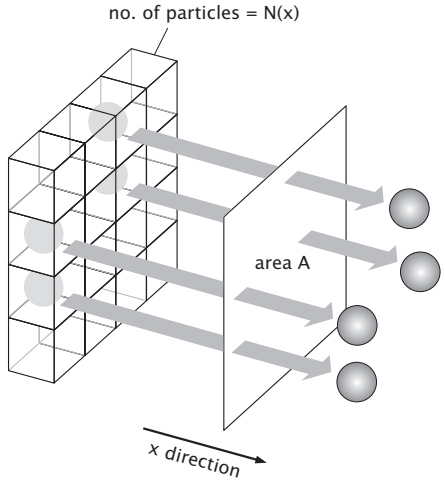

Figure 13.19: Flux due to an applied force. All the particles are moving with a drift velocity v to the right, resulting in $\Delta N = cv\Delta tA$ particles crossing the surface of area A in time Δt. The flux through the surface is $\Delta N/\Delta tA = cv$.

illustrated in fig. 13.19, results in a flux of the form

$$J_F = \frac{(v\Delta t)c}{\Delta t} = \frac{F}{\gamma}c. \tag{13.55}$$

We are now in the position to write the total flux as a sum of those parts due to random hopping and those parts due to the applied force. In particular, the total flux takes the form

$$J(x) = -D\frac{dc}{dx} + \frac{F}{\gamma}c. \tag{13.56}$$

Note that in equilibrium, the net flux vanishes, $J(x) = 0$, resulting in

$$D\frac{dc}{dx} = \frac{F}{\gamma}c. \tag{13.57}$$

This differential equation describes the way in which a nonuniform concentration distribution can be set up by the presence of a force and will be used, for example, to characterize the distribution of ions near a membrane. To explore the consequences of this result, we must first solve this simple linear differential equation which we can do using the separation of variables technique. Indeed, separation of variables results in

$$\gamma D\frac{dc}{c} = F dx. \tag{13.58}$$

It is convenient at this point to restrict our attention to those forces that can be derived from a potential energy as $F = -dU/dx$. As a result, we have

$$\gamma D \frac{dc}{c} = -dU. \tag{13.59}$$

This equation can be integrated to yield,

$$\frac{c(x)}{c(0)} = \frac{e^{-U(x)/\gamma D}}{e^{-U(0)/\gamma D}}. \tag{13.60}$$

This is exactly what we would expect from the Boltzmann distribution provided we set

$$D = k_B T/\gamma, \tag{13.61}$$

which is precisely the Einstein relation!

The Einstein relation is remarkable. It relates two quantities, diffusion and friction, which at first glance might seem worlds apart. The diffusion constant surmises the random motion of a microscopic particle through a fluid due to thermal agitation by the surrounding molecules. The friction coefficient on the other hand talks about the macroscopic effect of resistance to motion through a fluid experienced by objects large and small. Still, since both of these effects depend on the interaction of the particle with the molecules of the surrounding fluid, one might expect that there would be a relation between the two. In fact the experiments of Jean Perrin, inspired by Einstein's and Langevin's work on diffusion, ushered in the modern atomic view of diffusion.

The case of diffusion with drift also has important consequences out of equilibrium. Like before, mass conservation tells us that

$$\frac{\partial c}{\partial t} = -\frac{\partial J}{\partial x}. \tag{13.62}$$

On the other hand, since the flux has an extra term, the resulting governing equation itself has a new term and is given by

$$\frac{\partial c}{\partial t} = D\frac{\partial^2 c}{\partial x^2} - \frac{F}{\gamma}\frac{\partial c}{\partial x}. \tag{13.63}$$

As will be shown in the remainder of the book, this governing equation is important for describing a range of processes involving both external forcing and diffusion simultaneously.

13.3 Diffusion to capture

Another interesting class of problems associated with diffusion which show up in a number of different settings are those in which we are interested in the rate at which some diffusing species arrive at a given point. For example, the

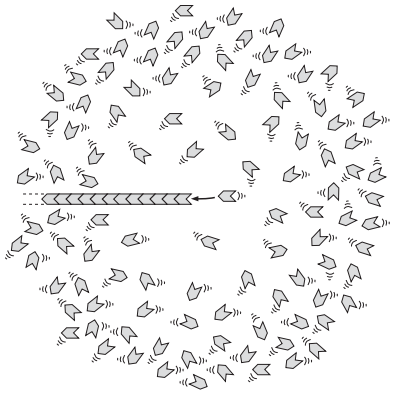

Figure 13.20: Monomer diffusion to the tip of a growing cytoskeletal filament. The figure illustrates that there is a depletion of monomers in the immediate vicinity of the growing tip. The schematic of the concentration profile around the filament ignores any disturbance to the distribution of monomers caused by the filament itself.

polymerization of cytoskeletal filaments such as actin require the arrival of unencumbered actin monomers at the tip of the growing filament as indicated schematically in fig. 13.20.

Similarly, a host of signaling processes depend upon the arrival of some mobile species of interest at the cell surface where they attach to some receptor and induce the resulting signal cascade. A generic representation of chemoreceptors on the cell surface is shown in fig. 13.21, though the idealization of uniform receptors shown in the schematic is a vast oversimplification (for example, see Kentner and Sourijk, 2006). The mathematical problem we are interested in solving in this case is illustrated schematically in fig. 13.22 in which we idealize a cell as a sphere and imagine a uniform distribution of receptor molecules that decorate the cell surface. In particular, we consider the case where there is a radial distribution of molecules centered around the cell and with a far field concentration c_0. The question we then pose is what is the rate at which molecules find their way to the surface receptors.

13.3.1 Modeling the cell signaling problem

We now make a concrete and mathematical description of the diffusion to capture process in the setting of the highly idealized geometry shown in fig. 13.22. As we have already mentioned, the goal of our calculation will be to compute the number of signaling molecules that bind to the receptors per unit time and represented mathematically as $\frac{dn}{dt}$. We assume the cell is a sphere of radius a which has M receptors on its surface. Further, we assume that the concentration profile has spherical symmetry ($c(\vec{r}) = c(r)$) and that there is a far field

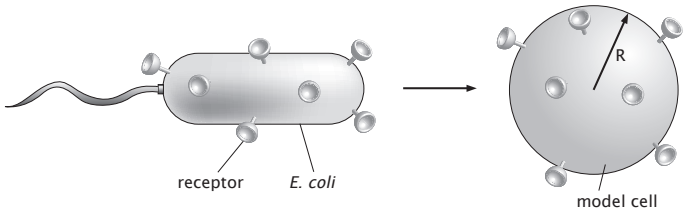

Figure 13.21: Cartoon representing the chemoreception process. The cell surface is peppered with receptors. For the purposes of simple analytical calculation, we idealize a bacterium as a sphere with a uniform density of receptors.

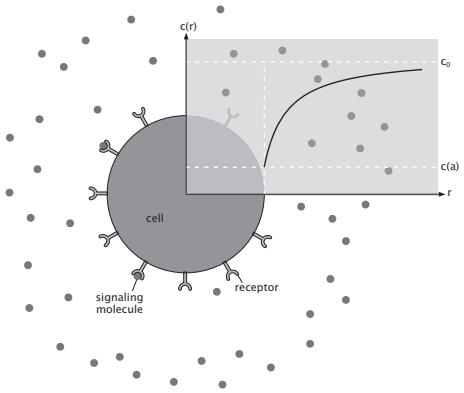

Figure 13.22: Concentration profile in the neighborhood of a spherical cell. The concentration profile $c(r)$ is spherically symmetric and characterizes the concentration of ligands as a function of distance from the cell surface.

concentration of signaling molecules $c_0 = c(\infty)$.

Perfect Receptors Result in a Rate of Uptake $4\pi D c_0 a$

In order to solve the problem using the *diffusion equation* we interest ourselves in the steady state condition characterized by $\frac{\partial c}{\partial t} = 0$. In this case, the diffusion equation given in eqn. 13.8 reduces to

$$D\nabla^2 c = 0. \tag{13.64}$$

For the special case of spherical symmetry, the Laplacian can be written only in terms of the radial variables and results in a simplification of the diffusion equation to the form

$$\nabla^2 c = \frac{1}{r^2}\frac{\partial}{\partial r}\left(r^2 \frac{\partial c}{\partial r}\right) = 0. \tag{13.65}$$

Since if the derivative of something is zero this implies that the something itself is a constant, we may rewrite this equation as

$$r^2 \frac{\partial c}{\partial r} = A \tag{13.66}$$

where A is a constant to be determined by the two boundary conditions: $c(a) = 0$ and $c(\infty) = c_0$. The condition $c(a) = 0$ amounts to asserting that the receptors on the cell surface are perfect absorbers. That is, all molecules that arrive at the surface are swallowed up by the receptors. Our strategy unfolds as follows. First, we use the diffusion equation to determine the concentration profile $c(r)$. This can be worked out explicitly by recognizing that the solution to eqn. 13.66 is given by

$$c(r) = -\frac{A}{r} + B, \tag{13.67}$$

which is obtained by integrating eqn. 13.66. By imposing the conditions that $c(a) = 0$ (perfect receptors) and $c(\infty) = c_0$, we can rewrite the concentration profile as

$$c(r) = c_0(1 - \frac{a}{r}). \tag{13.68}$$

Once the concentration is in hand, we can then use Fick's law to relate it to a current density. In particular, the flux at the surface of the cell is $j(a) = -D\partial c/\partial r|_a$, which is given by

$$j(a) = -\frac{Dac_0}{r^2}. \tag{13.69}$$

If we take this current density and multiply by the area of the sphere, what results is the total number of particles arriving per unit time and given by

$$\frac{dn}{dt} = -j(a)4\pi a^2 = 4\pi D a c_0. \tag{13.70}$$

This simple result, namely, $dn/dt = 4\pi D a c_0$ is one of the most useful interpretative tools for examining the rates of reactions ranging from receptor mediated

signaling to polymerization at the tip of a growing cytoskeletal filament. In particular, it is the basis of our ability to distinguish diffusion-limited and reaction rate limited reactions.

A Distribution of Receptors Is Almost as Good as a Perfectly Absorbing Sphere

In essence, the previous calculation assumed that no matter how fast diffusion delivers fresh ligands to the surface-bound receptors, they are prepared to take up those ligands. What happens in the case where the rate of uptake at the receptors is not fast enough to keep up with diffusion? To explore this, we assume that the cell has finite rate of signaling molecule adsorption, k_{on}. Note that we will recover our previous result in the limit that k_{on} is sufficiently large. The number of molecules adsorbed per unit time will be given by the rate equation

$$\frac{dn}{dt} = Mk_{on}c(a), \tag{13.71}$$

where M is the number of surface-bound receptors. The essence of the argument we pursue is that in steady-state a concentration profile will be established which guarantees that the diffusive flux is just large enough to feed the receptor adsorption process. Note that using mass conservation, the flux across an imaginary sphere at any radius is given by $-j(r)4\pi r^2$. The minus sign is present because the current density is defined to be positive when it points outward. If we use Fick's law together with eqn. 13.71 we get

$$-j(r)4\pi r^2 = D\frac{\partial c}{\partial r}4\pi r^2 = Mk_{on}c(a) \tag{13.72}$$

which can be written in integrated form as

$$\int_{c(a)}^{c(r)} dc = \int_a^r \frac{Mk_{on}c(a)}{4\pi D\, r^2}\, dr. \tag{13.73}$$

After integrating both sides we obtain

$$c(r) - c(a) = \frac{Mk_{on}c(a)}{4\pi Da} - \frac{Mk_{on}c(a)}{4\pi Dr}. \tag{13.74}$$

Finally, if we use the condition $c(\infty) = c_0$ the concentration at the cell's surface can be written as

$$c(a) = \frac{c_0}{1 + \frac{Mk_{on}}{4\pi Da}}. \tag{13.75}$$

There are two interesting limits to this expression and each one implies something different about $c(a)$. The first limit of interest corresponds to

$$\frac{Mk_{on}}{4\pi Da} \gg 1 \Rightarrow c(a) = 0. \tag{13.76}$$

Note that we have recovered the limit of perfect absorbers considered earlier in this section. This result implies that the receptors will be able to adsorb

signaling molecules as fast as diffusive processes can deliver them. The other limit corresponds to

$$\frac{Mk_{on}}{4\pi D\, a} \ll 1 \Rightarrow c(a) = c_0, \tag{13.77}$$

and implies that the on rate is so slow that the background concentration is not depleted at all.

The condition in eqn. 13.76 means that there is a maximum on rate even for a surface which is a perfect adsorber. This is precisely the on rate found in the previous discussion. However, this raises an interesting biological design question. What it says, more precisely, is that decorating a cell surface with too many receptors adds nothing further to the ability of that surface to take on board further ligands. To state this issue more precisely, we ask: how many receptors do we need before we have a situation almost as good as a fully adsorbing surface? Plugging in the result from eqn. 13.75 and assuming we have M receptors on the cell's surface

$$\frac{dn}{dt} = Mk_{on}c(a) = M\frac{k_{on}c_0}{1+\frac{Mk_{on}}{4\pi D\, a}} = \frac{4\pi D\, a\frac{Mk_{on}}{4\pi D\, a}c_0}{1+\frac{Mk_{on}}{4\pi D\, a}} \tag{13.78}$$

This result can be used to ask how many receptors we need on the surface in order to get an absorption rate which is half that of the diffusive speed limit given by $4\pi Dac_0$, for example. This condition amounts to solving the equation

$$\frac{dn}{dt} = \frac{4\pi D\, a\, c_0}{2} = \frac{\frac{Mk_{on}}{4\pi D\, a}4\pi D\, a\, c_0}{1+\frac{Mk_{on}}{4\pi D\, a}}, \tag{13.79}$$

for the parameter M. More precisely, this amounts to solving the equation

$$\frac{1}{2} = \frac{\beta}{1+\beta}, \tag{13.80}$$

where $\beta = \frac{Mk_{on}}{4\pi D\, a}$. The solution to the equation is $\beta = 1$ which implies

$$M = \frac{4\pi D\, a}{k_{on}}. \tag{13.81}$$

To see what this solution really means, we now resort to particular numerical examples. We consider a 'typical' eukaryotic cell which we idealize as a sphere of radius $a \simeq 10$ μm. Further, we assume a diffusion coefficient for the ligand species of 100 $\mu\mathrm{m}^2/\mathrm{s}$ and a $k_{on} \simeq 10$ $\mu\mathrm{M}^{-1}\mathrm{s}^{-1}$, which is the typical on rate for actin or parM polymerization. Before we proceed we have to turn the concentration in k_{on} into useful units, namely,

$$1\mu\mathrm{M} = \frac{6\cdot 10^{23}\cdot 10^{-6}}{\mathrm{L}} = 600/\mu\mathrm{m}^3. \tag{13.82}$$

Using eqn. 13.81, we can now compute $M \approx 10^5$ receptors.

It is interesting to consider whether or not 10^5 receptors on the surface of a cell with radius 10 μm is large or not. One measure of how crowded this distribution of receptors is can be garnered by computing the mean spacing, d, and the fraction of the surface that will be covered by these receptors. The surface area of the sphere (i.e. the cell) is $A_{sphere} = 4\pi(10\ \mu\text{m})^2 \approx 12 \cdot 100\ \mu\text{m}^2$. The mean spacing can then be estimated as

$$d^2 = \frac{12 \cdot 100\ \mu\text{m}^2}{10^5} = 12 \cdot 10^3\ \text{nm}^2 \simeq 100\ \text{nm} \cdot 100\ \text{nm}, \tag{13.83}$$

which says that the average spacing between receptors will be 100 nm. We can also ask what fraction of the area of the membrane is actually taken up by these receptors. If we consider a receptor with an area $b = 10\ \text{nm}^2 = 10^{-5}\ \mu\text{m}^2$, the fraction of the membrane area taken up by receptors is

$$\text{Covered membrane fraction} = \frac{10^5 \cdot 10^{-5}\ \mu\text{m}^2}{1200\ \mu\text{m}^2} = \frac{1}{1200}. \tag{13.84}$$

Interestingly, these simple estimates demonstrate that even a relatively sparse distribution of membrane-bound receptors can rival a perfectly absorbing sphere. Further, this estimate also reveals that many different species of receptor can decorate the cell surface simultaneously while leaving room for the others and with all receptors operating nearly as perfect absorbers.

13.3.2 A "Universal" Rate for Diffusion-Limited Chemical Reactions

The ideas about diffusion to capture introduced in the previous section have a very interesting application to the analysis of the rates of chemical reactions. We focus on a simple bimolecular reaction of the form $A+B \rightleftharpoons AB$. We imagine that the overall reaction rate is a conspiracy of two distinct factors. First, the overall rate of reaction clearly depends upon how often reactants arrive in each others vicinity as a result of diffusion. However, proximity is not necessarily a guarantee of reactivity. Once A and B have found each other, it may take many tries for them to join up to form AB. The argument we make here is that these two effects can result in limiting scenarios known as 'diffusion-limited reaction' and 'rate-limited reaction'. For the moment, we examine the case in which once the reactants are nearby, they react. The point of the exercise is to compute the universal speed limit for such diffusion-limited reactions.

One of the schemes we will return to for determining the rates of biological processes is to bound the rate of a given process on the assumption that its rate is dictated entirely by diffusion. For example, we can estimate the time it takes for capsid proteins to form a viral capsid by working out the diffusion time for individual proteins to be captured by the growing capsid. Of course, in reality many of the processes of interest involve several steps including that i) the relevant molecular participants find each other (both in terms of spatial position and orientation) and ii) once they do find each other, there is still some

energy barrier to traverse which slows down the rate. The idea advanced here is that the diffusive rate provides a maximum rate speed limit. Examples of interest include: the reaction $H^+ + OH^- \rightarrow H_2O$, the binding of oxygen to hemoglobin, the binding of *lac* repressor to DNA and the assembly of individual monomeric units to form viral capsids. The outcome of the most naive diffusive arguments (and in the case where the two diffusing particles are treated as being of the same size) is that the rate constant for molecular association is given by

$$k_{\text{diffusive}} = \frac{8k_BT}{3\eta}, \tag{13.85}$$

where η is the viscosity of the medium. This is simply obtained from eqn. 13.70 by replacing D with $2D$ and a with $2a$, to account for the mutual diffusion of two particles with equal diffusion constants, $D = k_BT/6\pi\eta a$, and the fact that they need to be within distance $2a$ to interact. If we use the numbers for water at room temperature to determine the viscosity ($\eta \approx 10^{-3}$ Pa s), this results in the value $k_{\text{diffusive}} \approx 7\times10^9$ M^{-1} s^{-1}, a value which is helpful for estimating rates for point-like particles, but overestimates the rates associated with protein-ligand interactions, a shortcoming that can be amended by acknowledging that a ligand can only interact correctly with its receptor in certain precise orientations. In this case the rotational diffusion of the ligand and the protein receptor must also be taken into account.

13.4 Summary and Conclusions

Because so many of life's processes occur at the molecular scale, the thermally driven diffusion of molecules is a major influence governing how rapidly and at what location biochemical reactions can occur. In this chapter we have examined several of the interesting dynamic consequences of the diffusive behavior of molecules. Diffusion as a transport mechanism is efficient over short, but not over long distances. As a mechanism for delivering ligands to receptors, the dynamics of diffusion generates a built in limit such that sparsely distributed receptors on a cell surface are nearly as efficient at receiving signals as a surface completely covered with receptors would be. We have also considered the consequences of allowing other processes to influence diffusive behaviors such as in the case of an external applied force or in the context of diffusion to capture. A remarkable number of cases in biological dynamics are well approximated by one of these simple scenarios. Reconciling the diffusive behavior of individual molecules with the macroscopic evolution of concentration gradients reveals one of the many fascinating ways that apparently directed behaviors at a macroscopic scale can arise from individually random and uncoupled behaviors of molecules. Diffusion is a fact of life at molecular scales; all molecular processes must either exploit diffusion or overcome it.

13.5 Problems

1. Biological distances and diffusion times.

Generate a series of plots like that shown in fig. 13.4 for all three choices of diffusion constant shown in table 13.1. Justify these choices of diffusion coefficients by using the Stokes relation $D = k_B T/6\pi\eta a$.

2. Diffusion from a point source.

The idea in this problem is to derive the solution to the one-dimensional diffusion equation for a point source, given by eqn. 13.32. The tools we invoke in this problem may seem heavy handed on the first try, but illustrate a bevy of important ideas from mathematical physics.

(a) Take the Fourier transform of the diffusion equation by transforming in the spatial variables to obtain a new differential equation for $\tilde{c}(k,t)$.
(b) Solve the resulting differential equation for $\tilde{c}(k,t)$. Then compute the inverse Fourier transform to arrive at the solution in real space $c(x,t)$.
(c) Show that the solution for an arbitrary initial concentration distribution $c(x,t=0)$ can be written as an integral over the solution for a point source. In particular, consider the case of a half space and find the resulting diffusive profile.
(d) Formally derive the relation $\langle x^2 \rangle = 2Dt$.

3. FRAP of one-dimensional *E. coli* revisited.

Fig. 13.16(A) shows different snapshots of an *E. coli* cell after it has been subjected to photobleaching. Use the solution for the FRAP problem of a one-dimensional bacterium (i.e. eqn. 13.47) to produce a plot of the difference between the initial concentration (i.e. before photobleaching) and the concentration at time t as shown in fig. 13.16(B). Make a series of plots for different time points using a diffusion constant for GFP in *E. coli* of $D = 7\ \mu\text{m}^2/\text{s}$.

4. Two-Dimensional FRAP Analysis

The goal of this problem is to generalize the one-dimensional treatment of FRAP given in the chapter. Consider a cell as a planar circle of radius R uniformly covered with freely diffusing fluorescent proteins. Imagine that the laser photo-bleaches a hole of radius a in the middle of the cell. Work out the concentration of fluorescent proteins in the cell as a function of position and time in analogy with the one-dimensional treatment of the problem done in the chapter. Compute the number of molecules in the hole after photobleaching as a function of time and compare it to the result obtained from the one-dimensional model.

5. Rotational diffusion

(a) Consider a sphere of radius R in water. Due to random collisions with the water molecules the sphere will rotationally diffuse. The diffusion law in this case is analogous to the one obtained for translational motion,

$$\left\langle \Delta\theta^2 \right\rangle = 2D_r t. \tag{13.86}$$

What are the units of the rotational diffusion coefficient D_r? Write down the formula for D_r using the Einstein relation and the rotational friction coefficient obtained in problem 10. 3, and convince yourself that the units are correct.
(b) Estimate how long it takes for an *E. coli* to diffuse over an angle equal to 1 radian. What is the distance traveled by the bacterium during that time?

6. Diffusion to capture and the diffusive speed limit.

In the chapter, we solved the problem of diffusion to capture using physical arguments to bypass explicitly solving the diffusion equation. In this problem we do the math.
(a) Write the diffusion equation for the perfect absorber case in spherical coordinates. Use the method of separation of variables and reproduce the solution given in the chapter.
(b) Use the flux to compute the number of molecules absorbed per unit time and find the corresponding k_{on} implied by this solution. Plug in reasonable numbers to compute the diffusive speed limit for the case of oxygen binding to hemoglobin.

7. Chemoreceptor clustering.

There is strong evidence that chemoreceptors in *E. coli* tend to cluster near one pole (see Kentner and Sourijk, 2006). One hypothesis about the role of such clustering is that it might increase the ability of a bacterium to better detect molecules in its environment. Determine if this is the most efficient strategy for counting (adsorbing) molecules of chemoattractant. Approximate *E. coli* as a sphere $a = 1$ μm in radius and neglect its motion. Then compare the diffusive current to $N = 1000$ receptors (adsorbing patches of radius $s = 10$ $\mathring{A}$) scattered over the surface of the cell to the diffusive current to the same receptors incorporated into a single patch with the same total area. Make use of the result that the diffusive current onto a sphere of radius a with N absorbing patches of radius s spread uniformly over its surface is

$$I = \frac{4\pi D c_\infty}{1 + \pi a/Ns}$$

where D is the diffusion constant of the molecules, while c_∞ is their concentration far from the cell. (Adapted from a problem courtesy of Howard C. Berg.)

13.6 Further Reading

D. Bray, **Cell Movements: From Molecules to Motility**, Garland Publishing, New York: New York, 2001. Bray's book is a beautiful description of a

host of dynamical processes associated with cells.

H. Berg, **Random Walks in Biology**, Princeton University Press, Princeton: New Jersey, 1993. Berg's book is a classic, but not in the sense of Mark Twain who quipped that a classic is something that is talked about by all and read by none. Berg's book is widely read and deservedly so.

H. Berg, *E. coli* **in Motion**, Springer, New York: New York, 2003. Another Berg classic!

G. B. Benedek and F. M. H. Villars, **Physics With Illustrative Examples from Medicine and Biology: Statistical Physics**, Springer-Verlag, Inc., New York: New York, 2000. Benedek and Villars have made their way to our "Further Reading" list in many chapters because they have interesting things to say on many topics.

J. Perrin, **Atoms**, Ox Bow Press, Woodbridge: Connecticut, 1990. This book is full of interesting insights to reward the curious reader.

A. Einstein, **Investigations on the Theory of the Brownian Movement**, Dover Publications Inc., New York: New York, 1956. Einstein's treatment of diffusion still serves as a fine introduction.

S. Chandrasekhar, "Stochastic Problems in Physics and Astronomy", Rev. Mod. Phys. **15**, 1 (1943). Chandrasekhar's amazing article is a compendium of elegant and useful results pertaining to random walks and more general ideas on stochastic processes.

D. Axelrod, D. E. Koppel, J. Schlessinger, E. Elson and W. Webb, "Mobility Measurement by Analysis of Fluorescence Photobleaching Recovery Kinetics", Biophys. J., **16**, 1055 (1976). This paper describes the theoretical underpinnings of the use of photobleaching as a tool to study dynamics within cells.

J. Lippincott-Schwartz, E. Snapp and A. Kenworthy, "Studying Protein Dynamics in Living Cells", Nat. Rev. Mol. Cell Biol. **2**, 444 (2001). An excellent account of the use of techniques such as FRAP for studying dynamics within cells.

A. S. Verkman, "Solute and macromolecule diffusion in cellular aqueous compartments", Trends in Biochem. Sci., **27**, 27 (2002). This article describes the use of photobleaching as a tool to study dynamics in living cells.

H. C. Berg and E. M. Purcell, "Physics of chemoreception", Biophys. J., **20**, 193 (1977). One of the classic papers in physical biology illustrating how ideas about diffusion to capture can be used to think about cell signaling.

D. Kentner and V. Sourijk, "Spatial organization of the bacterial chemotaxis system", Curr Opin Microbiol. **9**, 619 (2006). This paper demonstrates that the idea of uniformly distributed receptors is not appropriate for the chemotaxis system and that the receptors are localized to the poles.

13.7 References

J. Ellenberg, E. D. Siggia, J. E. Moreira, C. L. Smith, J. F. Presley, H. J. Worman and J. Lippincott-Schwartz, "Nuclear Membrane Dynamics and Reassembly in Living Cells: Targeting of an Inner Nuclear Membrane Protein in Interphase and Mitosis", J. Cell Biol. **138**, 1193 (1997).

M. B. Elowitz, M. G. Surrettee, P.-E. Wolf, J. B. Stock and S. Leibler, "Protein Mobility in the Cytoplasm of *Escherichia coli* ", J. Bacteriol. **181**, 197 (1999).

W.F. Marshall, A. Straight, J.F. Marko *et al.*, "Interphase chromosomes undergo constrained diffusional motion in living cells", Current Biology **7**, 930 (1997).

C. W. Mullineaux, A. Nenninger, N. Ray and C. Robinson, "Diffusion of Green Fluorescent Protein in Three Cell Environments in *Escherichia Coli*", J. Bacteriol. **188**, 3442 (2006).